Engineering 3 (2017) 641–647

Contents lists available at ScienceDirect

Engineering

journal homepage: www.elsevier.com/locate/eng

Research
Intelligent Manufacturing—Article

An Intelligent Non-Collocated Control Strategy for Ball-Screw Feed Drives with Dynamic Variations

Hui Liu [a,b], Jun Zhang [a], Wanhua Zhao [a,b,*]

[a] State Key Laboratory for Manufacturing Systems Engineering, Xi'an Jiaotong University, Xi'an 710054, China
[b] Collaborative Innovation Center of High-End Manufacturing Equipment, Xi'an Jiaotong University, Xi'an 710054, China

ARTICLE INFO

Article history:
Received 27 March 2017
Revised 24 May 2017
Accepted 13 June 2017
Available online 26 September 2017

Keywords:
Ball-screw feed drives
Varying high-order dynamics
Non-collocated control
Modal characteristic modifier
Intelligent adaptive tuning algorithm

ABSTRACT

The ball-screw feed drive has varying high-order dynamic characteristics due to flexibilities of the slender screw spindle and joints between components, and an obvious feature of non-collocated control when a direct position measurement using a linear scale is employed. The dynamic characteristics and non-collocated situation have long been the source of difficulties in motion and vibration control, and deteriorate the achieved accuracy of the axis motion. In this study, a dynamic model using a frequency-based substructure approach is established, considering the flexibilities and their variation. The position-dependent variation of the dynamic characteristics is then fully investigated. A corresponding control strategy, which is composed of a modal characteristic modifier (MCM) and an intelligent adaptive tuning algorithm (ATA), is then developed. The MCM utilizes a combination of peak filters and notch filters, thereby shaping the plant dynamics into a virtual collocated system and avoiding control spillover. An ATA using an artificial neural network (ANN) as a smooth parameter interpolator updates the parameters of the filters in real time in order to cope with the feed drive's dynamic variation. Numerical verification of the effectiveness and robustness of the proposed strategy is shown for a real feed drive.

1. Introduction

The ball-screw feed drive system exhibits high-order dynamics, and its dynamics vary with the position of the sliding carriage [1]. In addition to these varying high-order dynamics that are imposed on the motion and vibration control, another obvious feature of the feed drive, that is, non-collocated control when a direct position measurement using a linear scale is employed, makes it difficult to achieve a higher motion accuracy level for high-speed machine tools.

A non-collocated situation is present when the actuator and sensor (at the point of interest for control) are not placed on a single point or coordinate, which complicates the control problem because of the intervening dynamics involved [2,3]. Non-collocated control is closely related to the problems of out-of-phase modes [4], non-minimum phase (NMP) systems [5], and a transfer function with right-half-plane (RHP) zeroes [2]. These are all acknowledged as classical difficult-to-control problems in the field of motion and vibration control. It is believed that the source of the difficulty comes from the weak dynamics and limited wave propagation speed of the intervening structures. Various methods have been proposed to resolve this problem. Typical approaches include modal control [6,7], internal model control [8], delayed feedback control [9], zero phase error tracking control (ZPETC) [10], and modern control methods such as linear quadratic regulator (LQR) and linear quadratic Gaussian (LQG) methods [11]. It is also known that non-collocated systems have advantages over collocated systems; these include a high degree of observability and controllability, better high-frequency roll-off, and easy elimination of the high-frequency control spillover [4].

A great deal of research has been performed on feed drive control, and successful applications have been achieved on the high-speed control of ball-screw feed drives, considering the flexibilities

* Corresponding author.
E-mail address: whzhao@xjtu.edu.cn

http://dx.doi.org/10.1016/J.ENG.2017.04.007

and vibration of the ball-screw spindle [12,13]. Some of these works studied the effects of table position and load mass variation on the performance [14,15]. To deal with the varying dynamics, different approaches including classical adaptive control [6,16], robust control [17], and intelligent control [18] have been presented. However, little research has been reported on the study of feed drives from the aspect of the non-collocated system, even though the ball-screw feed drive is a typical non-collocated system and many successful methods and results [3,19] have been verified and could be utilized for such a study.

This study investigates the ball-screw feed drive from the aspect of a non-collocated system, after a brief description of the nature of a general non-collocated system. A corresponding control strategy, which is composed of a modal characteristic modifier (MCM) and an intelligent adaptive tuning algorithm (ATA), is then developed and applied to a practical ball-screw feed drive with varying high-order dynamics that have been modeled using a frequency-based dynamic substructure method. Finally, a numerical verification of the effectiveness and robustness of this strategy is shown.

The research reported in this paper is an extension of the author's work that is presented in Ref. [1]. The suggested control strategy, and particularly the use of a combination of peak filters and notch filters, is inspired by the practice in Ref. [6].

2. Non-collocated system control in ball-screw feed drives

A three-mass two-spring (3M2S) system, as shown in Fig. 1, was chosen as a simple example to illustrate the nature of a non-collocated system, along with the related difficulties for motion and vibration control. In a collocated situation, the actuator (which applies force or torque) and the sensor (which generates signals for feedback) are placed at a single point, such as the pair of F_1–x_1 (system h_{11}). In a non-collocated situation, the actuator and sensor are placed at different coordinates, such as the pairs of F_1–x_2 (system h_{21}) or F_1–x_3 (system h_{31}).

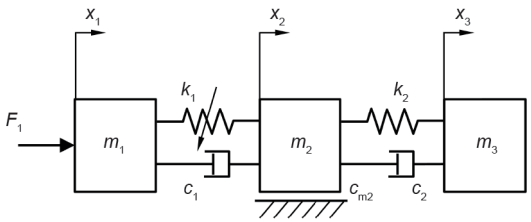

Fig. 1. Scheme of a 3M2S system. m_1, m_2, m_3 are the three masses; k_1 and k_2 are the two springs; c_1, c_2, and c_{m2} are the dampings; x_1, x_2, and x_3 are the displacements; and F_1 is the force applied on m_1.

Fig. 2 gives the frequency response functions (FRFs) for the 3M2S system, and Fig. 3 provides the derived operating deflection shapes of the rigid motion and two resonant modes for the 3M2S system. The parameter values used are m_1 = 100 kg, m_2 = 150 kg, m_3 = 50 kg, $k_1 = 5 \times 10^7$ N·m^{-1}, $k_2 = 2 \times 10^7$ N·m^{-1}, $c_1 = 1 \times 10^3$ N·s·m^{-1}, $c_2 = 4 \times 10^2$ N·s·m^{-1}, and $c_{m2} = 0$. It is clearly shown that for the collocated situation (h_{11}), the lag phase is always between 0° and 180°; for the non-collocated situation (h_{21}, h_{31}), the lag phases are much bigger, while the magnitude plots roll off much more sharply at the higher frequency band. The system of h_{11}, which is classified as a minimum phase system in classical control theory, is easy to control; the systems of h_{21} and h_{31}, which are non-minimum phase systems, are difficult to control, prone to instability, and sensitive to uncertainty.

Based on the deflection shapes in Fig. 3, it is observable that the coordinate of the actuator (Coordinate 1) has in-phase relations among the deflections of the rigid motion and of the two resonant modes. This is a desirable characteristic that ensures a definite stability using a simple feedback controller such as proportional-derivative (PD) control, which has a passive mechanical equivalence (Fig. 4). Unfortunately, non-collocated coordinates do not have this desirable feature. Their deflection shapes can be out of phase with the rigid motion, imposing conflict control requests on the controller. For example, for the non-collocated pair F_1–x_3, negative feedback should be used for rigid motion control and for vibration control of the second resonant mode (155 Hz), whereas positive feedback must be used for the first resonant mode (104 Hz). Simple control methods such as proportional-integral-derivative (PID) control cannot be used to settle this conflict.

A Nyquist plot provides another way to comprehend the nature of non-collocated systems (Fig. 5), and was used to develop a controller for non-collocated systems. In a Nyquist plot, a collocated system has all the circles, which denote resonant modes, positioned at one side, whereas a non-collocated system has circles at opposite sides. Nyquist plots thus hint at a control technique that involves modifying a non-collocated system to a virtual collocated one via phase adjustment. It should be noted that the following assumptions are implicitly used above: The modes are proportionally damped, the mode shape functions are real-valued, and there is no control delay or measure delay. If non-proportional damping or a time delay is considered, such as those that occur in practical feed drives, a simple in- or out-of-phase relation will no longer exist, and the non-collocated control problem will become more complex and difficult.

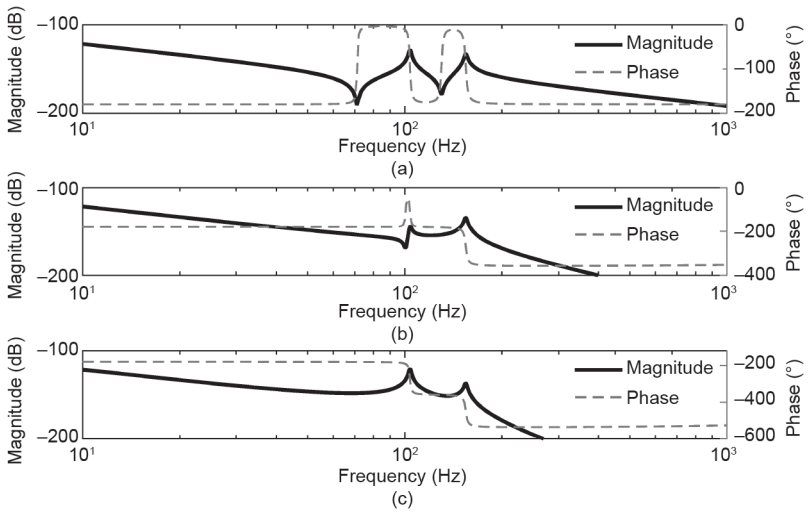

Fig. 2. FRFs of the 3M2S system. (a) h_{11}; (b) h_{21}; (c) h_{31}.

The structure of a ball-screw feed drive is illustrated in Fig. 6. A screw-nut couple connects the ball-screw and the sliding carriage, and transforms the ball-screw's rotation into the axial motion of the sliding carriage. The motor is connected to the ball-screw with a coupling. T_1, θ_1, and ω_1 are the torque applied on the rotor, rotational displacement, and velocity of the motor rotor (Coordinate 1), respectively; y_2 and v_2 are the axial displacement and velocity of the sliding component (Coordinate 2), respectively. When only the encoder at the motor end is used for feedback control, the system is collocated, and can easily be controlled with a high-gain simple controller. However, it is common for a linear scale attached at the base of the sliding component close to the working point (Coordinate 3) to be used for position feedback, so as to eliminate the negative effects of the clearance, flexible deflection, and thermal and pitch errors of the drive train. The sensor and actuator are non-collocated, and the intervening structure—that is, the drive train—has limited dynamics. Thus, the system becomes a non-collocated system that is difficult to control. In addition to the typical features described above, the non-collocated control of a ball-screw feed drive has some notable special features, which include: ① varying dynamics of the intervening structure; ② a time delay coming from limited control and measuring periods; and ③ a coordinate of ultimate interest (Coordinate 3) that is different from the sensor coordinate (Coordinate 2), with intervening dynamics between the coordinates that cannot be neglected.

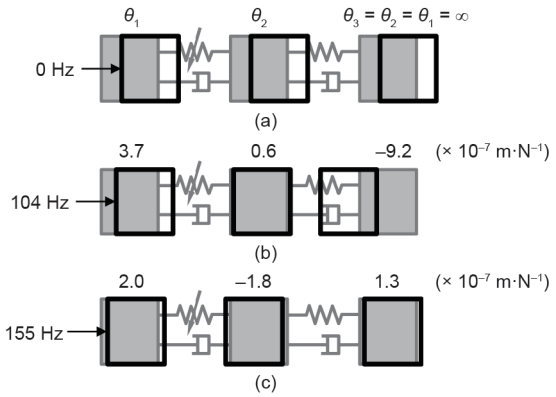

Fig. 3. Operating deflection shapes of the (a) rigid motion and (b,c) two resonant modes. θ_1, θ_2, and θ_3 are the receptances of the three coordinates.

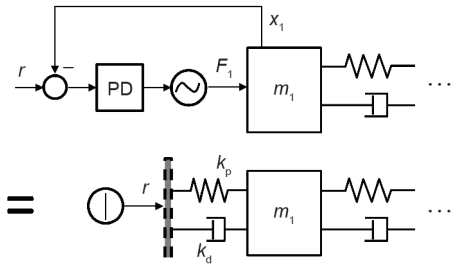

Fig. 4. PD collocated control and its passive mechanical equivalence. k_p: proportional gain; k_d: derivative gain; r: given displacement.

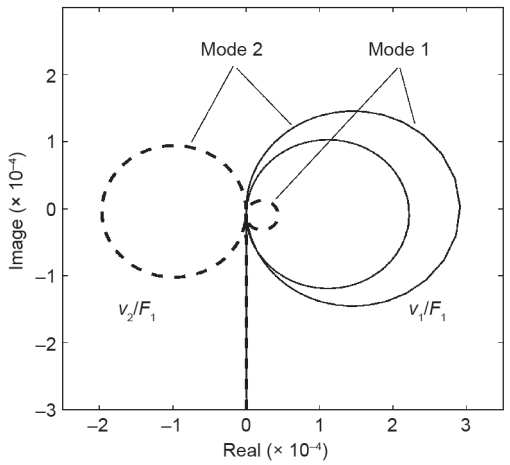

Fig. 5. Nyquist plots of collocated and non-collocated situations for 3M2S. v_1/F_1 and v_2/F_1 are the velocity receptances.

Fig. 7 introduces a general model that considers the features of non-collocated control for a ball-screw feed drive. In the model, the mechanical dynamics are a two-in tri-out FRF matrix H_{3x2} composed of h_{ij}; the motor is simplified as the gain $k_i k_T$, that is, the product of the current amplification and the torque constant; the control delay is simplified as a time lag τ; and the signal u, F_1, and F_3 (F_d) are the command acceleration, servo force, and disturbance force, respectively. This model is used for further controller development and for the integrated simulation. The model consists of the mechanical dynamics of two-in tri-out FRFs, the time delay effect, and a simplified model of the servo motor and its driver.

3. Varying high-order dynamic modeling of the plant

This section presents a brief introduction of the multi-subsystem receptance coupling method and the corresponding modeling approach for a ball-screw feed drive that are suggested by the author in Ref. [1], followed by illustrations of dynamic variation analysis based on the FRF model acquired.

3.1. Dynamic modeling

The ball-screw is considered to be a distributed-parameter system, taking into account its rotational and axial flexibility. The remaining elements, including bearings, coupling, motor rotor, and the sliding component, are assumed to be lumped-parameter. In the dynamic substructure method, the ball-screw feed drive is divided into three subsystems, as shown in Fig. 8: These include subsystem A,

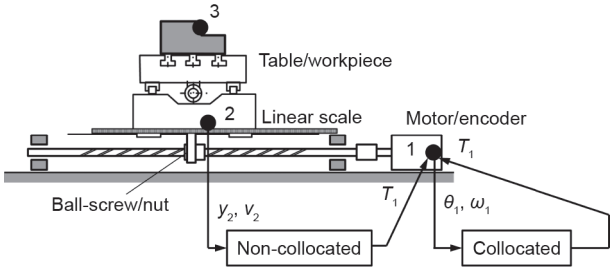

Fig. 6. Collocated and non-collocated control in ball-screw feed drives.

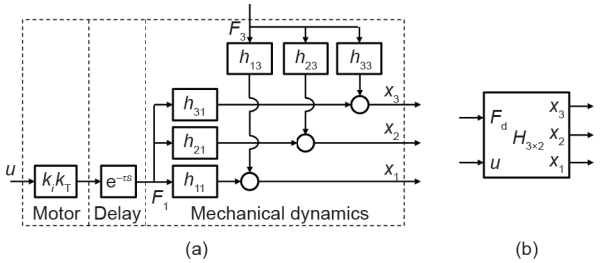

Fig. 7. (a) A general model considering the non-collocated situation and (b) its symbolic representation.

which consists of the rotational motion and vibration of the assembly of the ball-screw, the coupling, and the motor rotor with its rotational supports; subsystem B, which consists of the axial motion and vibration of the ball-screw with its axial supports; and subsystem C, which consists of the axial motion and vibration of the sliding component due to the carriage's axial and pitching movement.

Fig. 9 shows the schematic model of the proposed tri-subsystem receptance coupling via the screw-nut for a ball-screw feed drive. This model was used to connect (i.e., assemble) the three subsystems mentioned above.

Eq. (1) is the receptance coupling equation according to the subsystem linking configuration shown in Fig. 9, which connected the three subsystems via the screw-nut in order to acquire a coupled system:

$$\begin{bmatrix} h'_{a2a2} & h'_{a2c2} & h'_{a2c3} \\ h'_{c2a2} & h'_{c2c2} & h'_{c2c3} \\ h'_{c3a2} & h'_{c3c2} & h'_{c3c3} \end{bmatrix} = \begin{bmatrix} h_{a2a2} & 0 & 0 \\ 0 & h_{c2c2} & h_{c2c3} \\ 0 & h_{c3c2} & h_{c3c3} \end{bmatrix} - \begin{bmatrix} -\frac{h_{a2a1}}{i_a^b} \\ h_{c2c1} \\ h_{c3c1} \end{bmatrix} \left[\frac{h_{a1a1}}{(i_a^b)^2} + h_{b1b1} + h_{c1c1} + \frac{1}{k_{ja} + ic_{ja}\omega} \right]^{-1} \begin{bmatrix} -\frac{h_{a1a2}}{i_a^b} \\ h_{c1c2} \\ h_{c3c1} \end{bmatrix}^T \quad (1)$$

where i and ω are the imaginary unit and angular frequency, respectively; h_{a1a1}, h_{b1b1}, h_{c1c2} … are the pre-coupling FRFs (receptances) of the subsystems; h'_{a2a2}, h'_{a2c2} … are the post-coupling FRFs of the connected system; i_a^b is the transmission ratio from the interface coordinate of subsystem A to that of subsystem B; and k_{ja} and c_{ja} are the equivalent axial stiffness and damping of the screw-nut joint surface, respectively.

The Newton-Euler equation and the conventional two-coordinate receptance equation were used in the ball-screw's rotational subsystem and axial subsystem modeling. Multi-rigid-body dynamic modeling, Laplace transformation, and complex matrix inversion were used for the sliding subsystem. Eq. (1) is used to connect the three subsystems. The final step of the proposed modeling approach is as follows:

$$H_M(Y_{table}) = \begin{bmatrix} h_{M11}(l) & h_{M13}(l) \\ h_{M21}(l) & h_{M23}(l) \\ h_{M31}(l) & h_{M33}(l) \end{bmatrix} = \begin{bmatrix} h_{R11} & 0 \\ 0 & h_{S23} \\ 0 & h_{S33} \end{bmatrix} - \begin{bmatrix} -\frac{h_{R1l}(l)}{i_{sc}} \\ h_{S21} \\ h_{S31} \end{bmatrix} \left[\frac{h_{Rll}(l)}{i_{sc}^2} + h_{All}(l) + h_{Snn} + \frac{1}{k_{ja} + ic_{ja}\omega} \right]^{-1} \begin{bmatrix} -\frac{h_{R1m}(l)}{i_{sc}} \\ h_{S13} \end{bmatrix}^T \quad (2)$$

where i_{sc} is the ball-screw's transmission ratio; k_{ja} and c_{ja} are the screw-nut's axial stiffness and damping, respectively; Y_{table} is the table's Y position displayed on the numerical control (NC) unit, where the nut location $l = Y_{table} + l_0$; the subscript M refers to the assembled mechanical system; the subscripts R, A, and S refer to the rotary subsystem, axial subsystem, and sliding subsystem, respectively; the subscripts 1, 2, and 3 refer to Coordinates 1, 2, and 3 as shown in Fig. 6; the subscripts n and l refer to the coordinate of the sliding carriage at the nut position and coordinate of the ball-screw at the nut position; and the subscript m refers to the coordinate of the motor rotor.

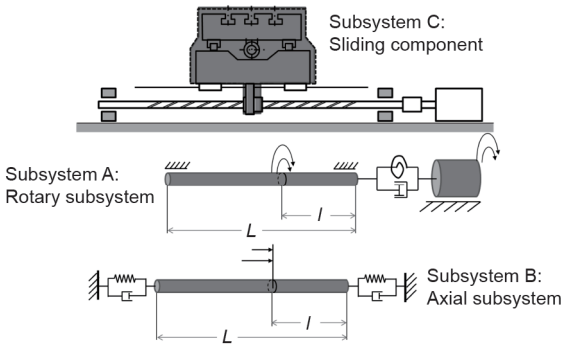

Fig. 8. Three subsystems of a ball-screw feed drive.

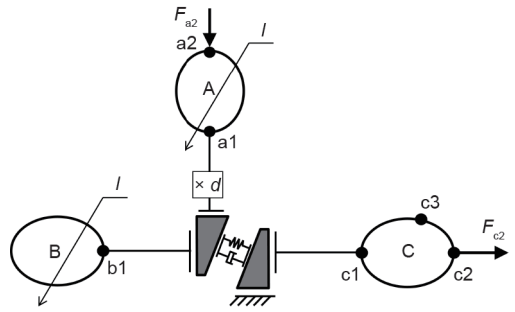

Fig. 9. Schematic model of the tri-subsystem receptance coupling via the screw-nut. Block "× d" stands for multiplication by the diameter of the ball screw.

3.2. Dynamic variation analysis

The proposed modeling approach has high computational efficiency and can be used for the position-dependent dynamic variation analysis. FRF variation can be predicted using the modeling approach directly: Fig. 10 illustrates the varying dynamics with families of magnitude plots, and Fig. 11 illustrates the varying dynamics in cloud images. It was determined from the predicted data that some of the frequencies and magnitudes are nearly constant for the varied table positions, while some resonant frequencies and magnitudes present notable and regular variation. It was also determined from the cloud images that higher frequency resonant modes exhibit much bigger variation than lower frequency modes.

The modal characteristics can be extracted from the FRFs and used to analyze the position-dependent dynamics of a ball-screw feed drive. The mode shapes are of special importance in comprehending the underlying nature of the different patterns of variation and in optimizing the structure while considering its dynamic variation. Phase variation is often neglected in related studies. However, the success of lead/lag compensation and peak filter control is contingent on the resonant phases and their variations. Fig. 12 shows the resonant phase variations of some modes. It was determined that, similar to the frequencies and magnitudes, some of the phase plots are nearly constant for the varied table positions while others present a notable variation, and that higher frequency resonance exhibits a much greater phase variation than lower frequency resonance. The phase values and their variation patterns suggest complex mode shapes of the practical feed drive system, whose coordinates do not have a simple in-phase or out-of-phase relation [20,21]. This is very important when modal control is used.

4. An intelligent non-collocated control strategy

This section proposes an intelligent non-collocated control strategy for a ball-screw feed drive system. Fig. 13 provides the control frame of the strategy. The main features of the strategy are as follows:

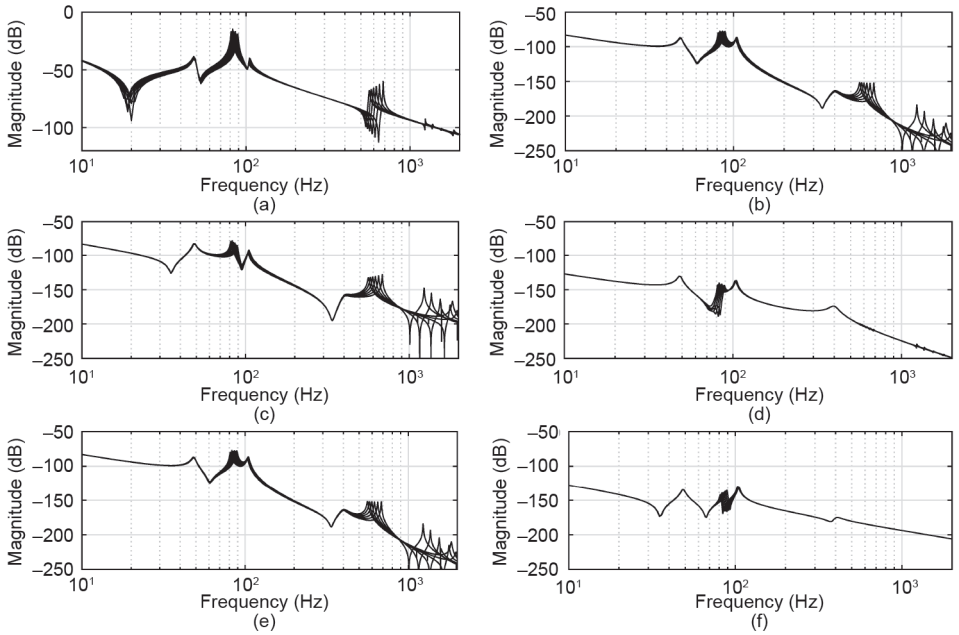

Fig. 10. Varying dynamics shown with families of magnitude plots (Y_{table} = 100–700 mm). (a) T_1 in and θ_1 out; (b) F_3 in and θ_1 out; (c) T_1 in and x_2 out; (d) F_3 in and x_2 out; (e) T_1 in and x_3 out; (f) F_3 in and x_3 out.

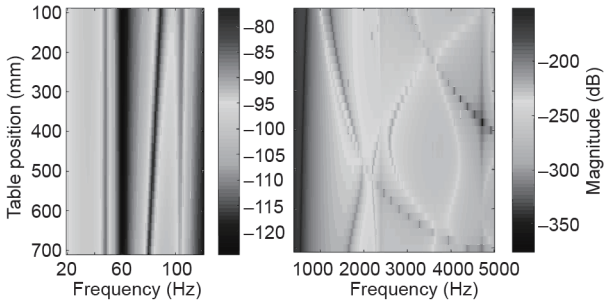

Fig. 11. Varying dynamics h_{21} shown with cloud images (Y_{table} = 100–700 mm).

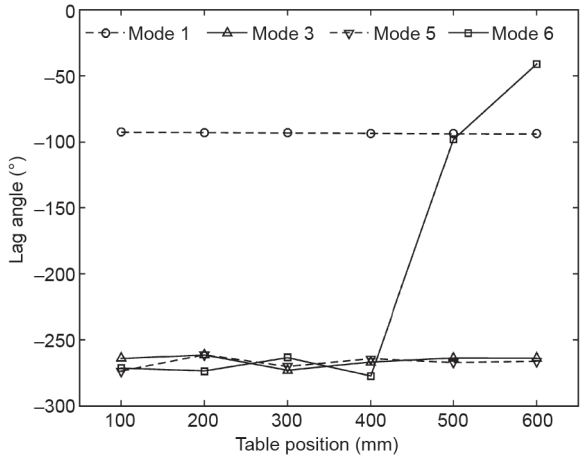

Fig. 12. Resonant phase variation with table position (h_{21}).

(1) A nested double-loop control frame is adopted. The inner loop is a collocated speed-control loop, while the outer is a non-collocated position-control loop. The differential operator s is used to generate velocity feedback from displacement measurement. The inner loop is used to supply control damping and modify the plant characteristic; the outer loop, using direct feedback, is used to achieve high position accuracy. Double-loop control also has the advantage of easy implementations of speed feed-forward and acceleration feed-forward control, that is, k_{ffv} and k_{ffa}.

(2) An MCM is added on the inner loop, which is a combination of peak filters (G_{pf1}, ..., G_{pfm}) and notch filters (G_{nf1}, ..., G_{nfn}); this is mainly used to correct the negative effects of the non-collocated system for the outer loop, and to remove the effects of high-frequency spillover.

(3) An ATA is designed to tune the parameters of the MCM; this generates smooth interpolated parameters according to the input position, based on the data from several fine-tuned local controllers.

4.1. Modal characteristic modifier

An MCM is a combination of peak filters and notch filters. The peak filters are used to modify the low-middle frequency modes to an in-phase or almost in-phase situation, which helps to increase the control gain of the speed-control loop and eliminate the negative effects of non-collocated control for the position-control loop. The notch filters are used to cancel the higher frequency modes in order to avoid control spillover. The use of a combination of filters, rather than the use of notch filters alone, has the advantages of low sensitivity to uncertainty and higher vibration resistance against cutting forces.

The peak filter part (G_{pf}) of an MCM is given by Eq. (3) [19]:

$$G_{pf} = 1+\sum_{i=1}^{m} K_i \frac{s(s\cos\varphi_i + \omega_i \sin\varphi_i)}{s^2 + 2\xi_i\omega_i s + \omega_i^2} \tag{3}$$

where s is the Laplace variable, m is the number of peak filters used, ω_i is the resonant frequency, ξ_i is the damping ratio, φ_i is the shift phase, and K_i is the gain.

Every peak filter has four parameters that can be tuned to modify a target mode. From a practical perspective, a peak filter in Eq. (3) performs two modifying effects on the mechanical modes: magnitude adjustment and phase shift. Fig. 14 illustrates these effects upon a target mode with varying characteristics. It is shown that the modified mode has higher open-loop gain and notably increased stability, which are of vital importance for higher motion- and vibration-

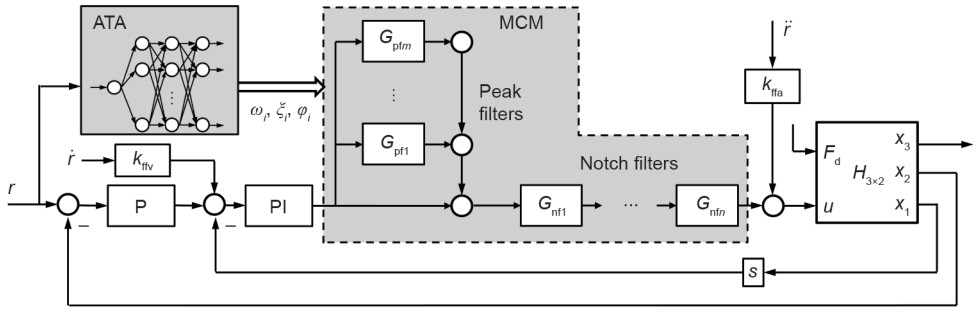

Fig. 13. The proposed intelligent non-collocated control strategy. P: proportional; PI: proportional-integral.

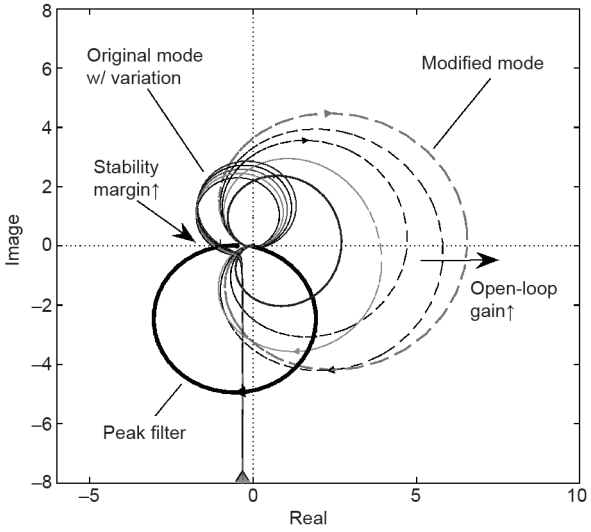

Fig. 14. Modifying effects of the proposed peak filter, where w/ variation refers to with variation.

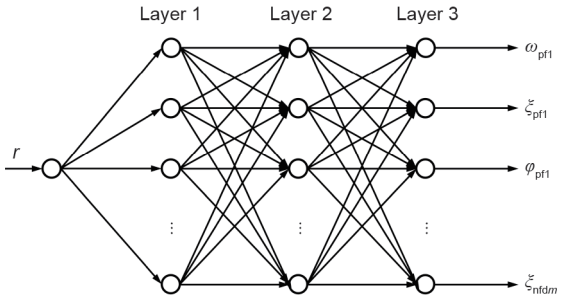

Fig. 15. The structure of the proposed ATA based on an ANN.

control performance.

Common second-order notch filters (G_{nf}) were used in the MCM, as shown in Eq. (4) [6]:

$$G_{nf} = \prod_{j=1}^{n} \frac{s^2 + 2\xi_{nj}\omega_j s + \omega_j^2}{s^2 + 2\xi_{dj}\omega_j s + \omega_j^2} \quad (4)$$

where n is the number of notch filters used, ω_j is the notched frequency, and ξ_{nj} and ξ_{dj} are the damping ratios.

4.2. Intelligent adaptive tuning algorithm

It is well known that the notch filter is very sensitive to the notch frequency. If the notch frequency is different than the actual resonant frequency, a closed-loop system may exhibit increased oscillation or even become unstable. The proposed peak filter (Eq. (3)) is robust to the frequency difference but sensitive to the actual resonant phase. Taking into account the notable position-dependent variation of the ball-screw feed drive's modal characteristics, an ATA is suggested here.

The preconditions for the ATA include: ① accurate modal characteristics of the plant for selected fixed table position, which are predicted based on a verified model or experimental analysis; and ② properly designed and fine-tuned local controllers, using numerical optimization or a manual tuning approach.

An artificial neural network (ANN) was chosen to realize the ATA; this generates smooth interpolated parameters according to the input position value, based on the data from several fine-tuned local controllers. Fig. 15 shows the structure of the proposed ATA based on an ANN, which has three layers: The first and second are the hidden layers, and the third is the output layer. The input of the network is the table position; the outputs are parameters for the filters in the MCM that are adaptive to the table position. The S-type transfer function and the linear function are used for the nodes of the hidden layers and output layers, respectively. The backpropagation (BP) algorithm is used to train the network.

5. Numerical simulation and verification

The proposed control strategy was applied to a practical ball-screw feed drive with position-dependent dynamics that were modeled and verified in Ref. [1]. Table 1 gives the modal characteristics identified from the FRF dynamic model. Utilizing Nyquist plots, modes were selected according to their effects on the stable margin. Mode 3 was selected as the target mode for the peak filter, and Mode 5 was selected for the notch filter ($n = m = 1$). To summarize, the MCM was designed to correct the phase of Mode 3 and cancel the resonance of Mode 5. Six fixed local controllers were tuned manually, maximizing the motion control performance, and were used to train the ANN. The ATA with the single-in seven-out ANN in this case was mainly used to adjust the filters' parameters in order to cope with the variation of the actual phase of Mode 3 and the actual frequency of Mode 5.

Fig. 16 and Fig. 17 provide the simulation results for the tracking responses and errors of a short-stroke reciprocating motion, under traditional PID control and the proposed control. It was found that the errors under the proposed control are much smaller and smoother than those under PID control. These benefits stem from the MCM helping to increase the loop gain. Fig. 18 provides a comparison of the root-mean-squared (RMS) errors and their variation. The jump in RMS error under PID control reflects the increasing vibration, which eventually becomes unstable when the table moves to the ball-screw end. This occurs when the PID parameters are too high. Again, it is shown that the proposed control achieved smaller RMS error and smaller variation than the PID control. These results and this comparison verify the effectiveness and robustness of the proposed control strategy.

Table 1
Modal characteristics identified for the test plant (Y_{table} = 115 mm).

Mode	Natural frequency (Hz)	Damping ratio	Phase (°)
1	49	0.120	−135
2	95	0.170	−155
3	130	0.090	−260
4	1030	0.003	−198
5	1529	0.010	−31

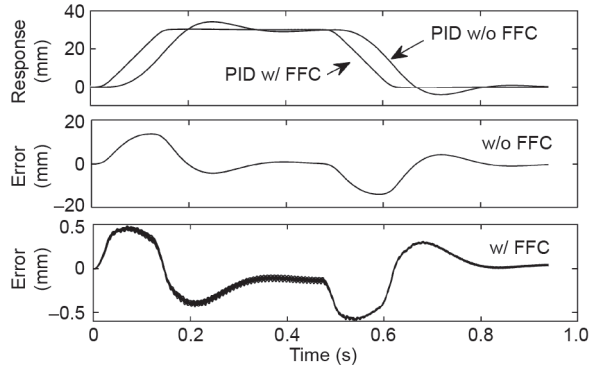

Fig. 16. Tracking responses and errors with PID control (Y_{table} = 115 mm), where w/ FFC refers to with feed-forward control and w/o FFC refers to without feed-forward control.

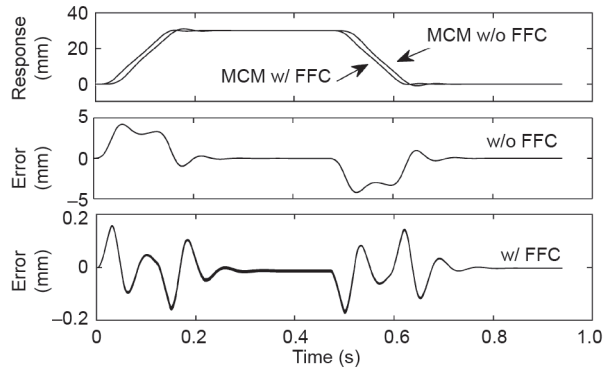

Fig. 17. Tracking responses and errors with the proposed MCM control (Y_{table} = 115 mm).

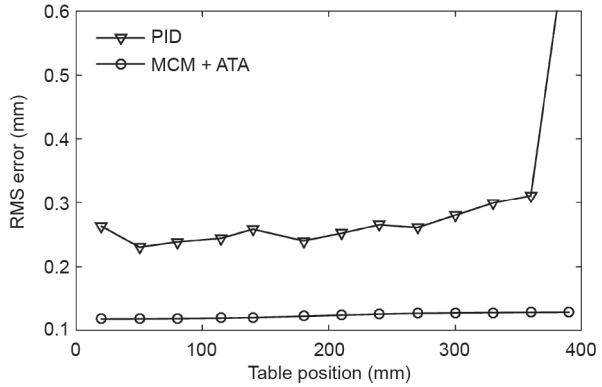

Fig. 18. An RMS error comparison.

6. Conclusions

A systematic investigation was performed on the non-collocated nature of ball-screw feed drive control. This paper presented a corresponding control strategy that is composed of an MCM and an intelligent ATA. The modifier utilized a combination of peak filters and notch filters, thereby shaping the plant dynamics into a virtual collocated system and avoiding control spillover. The ATA used an ANN as a smooth parameter interpolator, updating the parameters of the filters in real time to cope with the feed drive's dynamic variation. Numerical verification of the effectiveness and robustness of the proposed strategy was performed.

Acknowledgements

This work was supported by the key project of the National Natural Science Foundation of China (51235009).

Compliance with ethics guidelines

Hui Liu, Jun Zhang, and Wanhua Zhao declare that they have no conflict of interest or financial conflicts to disclose.

References

[1] Liu H, Lu D, Zhang J, Zhao W. Receptance coupling of multi-subsystem connected via a wedge mechanism with application in the position-dependent dynamics of ballscrew drives. J Sound Vib 2016;376:166–81.
[2] Chodavarapu PA, Spong MW. On noncollocated control of a single flexible link. In: Proceedings of the IEEE International Conference on Robotics and Automation; 1996 Apr 22–28; Minneapolis, USA. Piscataway: IEEE; 1996. p. 1101–6.
[3] Buhr C, Franchek MA, Bernhard RJ. Non-collocated adaptive-passive vibration control. J Sound Vib 1997;206(3):371–98.
[4] Kim SM, Oh JE. A modal filter approach to non-collocated vibration control of structures. J Sound Vib 2013;332(9):2207–21.
[5] Spector VA, Flashner H. Modeling and design implications of noncollocated control in flexible systems. J Dyn Sys Meas Control 1990;112(2):186–93.
[6] Wu S, Lian S, Chen S. Vibration control of a flexible beam driven by a ball-screw stage with adaptive notch filters and a line enhancer. J Sound Vib 2015;348:71–87.
[7] Mahmood IA, Moheimani SOR, Bhikkaji B. Precise tip positioning of a flexible manipulator using resonant control. IEEE/ASME Transactions Mechatronics 2008;13(2):180–6.
[8] Lee YS, Elliott SJ. Active position control of a flexible smart beam using internal model control. J Sound Vib 2001;242(5):767–91.
[9] Yang B, Mote CD. Active vibration control of the axially moving string in the S domain. J Appl Mech 1991;58(1):161–85.
[10] Torfs D, de Schutter J, Swevers J. Extended bandwidth zero phase error tracking control of non-minimal phase systems. J Dyn Sys Meas Control 1992;114(3):347–51.
[11] Han JH, Rew KH, Lee I. An experimental study of active vibration control of composite structures with a piezo-ceramic actuator and a piezo-film sensor. Smart Mater Struct 1997;6(5):549.
[12] Altintas Y, Verl A, Brecher C, Uriarte L, Pritschow G. Machine tool feed drives. CIRP Ann Manuf Technol 2011;60(2):779–96.
[13] Gordon DJ, Erkorkmaz K. Accurate control of ball screw drives using pole-placement vibration damping and a novel trajectory prefilter. Precis Eng 2013;37(2):308–22.
[14] Hanifzadegan M, Nagamune R. Tracking and structural vibration control of flexible ball-screw drives with dynamic variations. IEEE/ASME Transactions Mechatronics 2015;20(1):133–42.
[15] Zhou Y, Peng F, Li B. Adaptive notch filter control for the torsion vibration in lead-screw feed drive system based on neural network. In: Proceedings of the Intelligent Robotics and Applications, First International Conference, ICIRA 2008; 2008 Oct 15–17; Wuhan, China. Berlin: Springer; 2008. p. 803–12.
[16] Beauduin T, Fujimoto H, Terada Y. Adaptive vibration suppression perfect tracking control for linear time-varying systems with application to ball-screw feed drives. In: Proceedings of the International Workshop on Advanced Motion Control; 2016 Apr 22–24; Auckland, New Zealand. Piscataway: IEEE; 2016. p. 245–50.
[17] Itoh K, Iwasaki M, Matsui N. Robust fast and precise positioning of ball screw-driven table system on machine stand. In: Proceedings of the International Workshop on Advanced Motion Control; 2004 Mar 28; Kawasaki, Japan. Piscataway: IEEE; 2004. p. 511–5.
[18] Fernandez-Gauna B, Ansoategui I, Etxeberria-Agiriano I, Graña M. Reinforcement learning of ball screw feed drive controllers. Eng Appl Artif Intel 2014;30(1):107–17.
[19] Yabui S, Okuyama A, Atsumi T, Odai M. Development of optimized adaptive feed-forward cancellation with damping function for head positioning system in hard disk drives. J Adv Mech Design Sys Manuf 2013;7(1):39–51.
[20] He J, Fu ZF. Modal analysis. Oxford: Butterworth-Heinemann; 2001.
[21] Imregun M, Ewins DJ. Complex modes—Origins and limits. In: Proceedings of the 13th International Modal Analysis Conference; 1995 Feb 13–16; Nashville, USA. Bellingham: SPIE Press; 1995. p. 2460.